

Wideband trans-impedance amplifier with bandwidth tuning for near infra-red spectroscopy bio-medical applications

Muthukumar Balasubramanian, Ramachandran Balasubramanian

Department of Electronics and Communication Engineering, College of Engineering and Technology,
SRM Institute of Science and Technology, Kattankulathur, India

Article Info

Article history:

Received May 20, 2024

Revised Jul 30, 2024

Accepted Aug 6, 2024

Keywords:

Coarse grain tuning

Fine grain tuning

InvCas TIA

Near infra-red spectroscopy

Trans-impedance gain

Tunable bandwidth

Selectable bandwidth

ABSTRACT

A wide band trans-impedance amplifier (WBTIA) with tunable bandwidth for near infra-red spectroscopy (NIRS) bio-medical applications is presented in this research article. The first stage of the proposed WBTIA is implemented by a modified inverter-cascode (InvCas) trans-impedance amplifier (TIA) with series and shunt inductive peaking for the bandwidth extension and a common-source amplifier as a second stage for gain boosting. Bandwidth tuning is achieved by a novel tuning mechanism with a fixed capacitor and tunable metal-oxide-semiconductor (MOS) capacitor with a control voltage. The fixed capacitor provides a coarse-grain bandwidth tuning whereas the tunable MOS capacitors are used for fine-grain bandwidth tuning. The WBTIA is designed in 45 nm technology and it achieved a maximum trans-impedance gain (TIG) of 84.91 dBΩ and 354.81 MHz bandwidth. The proposed WBTIA consumes 41.24 μW power from 1 V supply voltage. The input referred current noise at 100 MHz is 169 fA/sqrt (Hz) and the output noise voltage is 69.8 pV/sqrt (Hz).

This is an open access article under the [CC BY-SA](https://creativecommons.org/licenses/by-sa/4.0/) license.



Corresponding Author:

Muthukumar Balasubramanian

Department of Electronics and Communication Engineering, College of Engineering and Technology,

SRM Institute of Science and Technology

Kattankulathur, Chennai-603203, Tamilnadu, India

Email: muthukub1@srmist.edu.in

1. INTRODUCTION

Trans-impedance amplifiers (TIA) are widely used in different varieties of biomedical instruments such as non-invasive blood glucose measurement, pulse-oximeters and cuffless-blood-pressure monitoring. Various bio-medical sensors require different gain and bandwidth combinations. A trans-impedance amplifier with a wide bandwidth and better gain is required to support different varieties of sensors with various bandwidth requirements. The proposed wide band trans-impedance amplifier (WBTIA) supports such requirements. Various design techniques and methodologies can be applied to attain the necessary gain and bandwidth for a specific near infra-red spectroscopy (NIRS) biomedical application. Different methods and materials were discussed in the literature.

A comparative study on complementary metal-oxide-semiconductor (CMOS) TIA topologies for different biomedical applications was discussed [1]. TIA are used for various bio-medical applications such as cuffless blood pressure measurement [2]–[4], noninvasive blood glucose level measurement [5], [6] hemoglobin measurement [7], brain function mapping [8], [9] and lung efficiency assessment [10]. A photodiode (PD) transforms optical power into a photo-current that is supplied to a trans-impedance amplifier that amplifies and converts the current signal into an output voltage-signal. Many TIA topologies are available in the literature review for various bio-medical applications. The specific application of the TIA is

based on the various performance parameters of the TIA such as the trans-impedance gain, bandwidth, input referred noise-current, output noise voltage, power, power supply, operating temperature, and dynamic range.

Various TIA topologies can be used to achieve the above-mentioned performance parameters based on the trade-off. A few TIA topologies such as common-source TIA [11], [12] Inverter TIA [13], [14] inverter cascode (InvCas) TIA [15], regulated inverter cascode TIA [16], and common-gate TIA [17]. are used in bio-medical applications. The bandwidth requirement of the TIAs used in bio-medical applications is between 5 kHz to 100 MHz. The bandwidth of the TIA can be tuned or varied by various techniques such as inductive peaking [18], MOS-Bipolar pseudo-resistor-based tuning [19], p-channel metal-oxide-semiconductor (PMOS) active resistor-based tuning [20], feedback resistor-based bandwidth tuning [21], load capacitor and photo-diode capacitor-based tuning [22] and bandwidth tuning by varying load-resistor [23]. Trans-impedance amplifiers are also used in high optical receivers [24]. High-gain op-amp [25] can also be used in biomedical application

The bandwidth tuning is accomplished by varying the load-capacitor and the input capacitance with novel capacitance tuning with coarse-grain and fine-grain tuning. The desired bandwidth selection is achieved by a tunable high-pass filter (HPF) with a lower cutoff-frequency and a low-pass filter (LPF) with a higher cutoff-frequency. Section 2 presents the proposed wideband TIA architecture. Section 3 deliberates the results and the conclusion of the paper is presented in section 4.

2. PROPOSED WIDEBAND TIA

The proposed wideband TIA with bandwidth tuning has four major blocks. The first block is the modified InvCas TIA, the second block is a buffer amplifier, the third block is a HPF and the last block is an LPF. Figure 1 illustrates the block schematic of the proposed WBTIA.

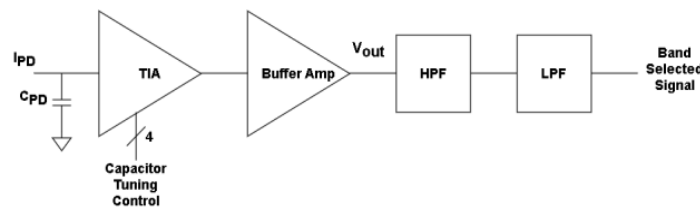


Figure 1. Block Schematic of the WBTIA

2.1. Proposed modified inverter-cascode TIA

An inverter-cascode trans-impedance amplifier (InvCas TIA) is a vital circuit of an optical-receiver that improves the specifications by reducing the limitations of the large photodiode-capacitance at the input-side of the circuit. It has high voltage gain, reduced Miller effect, better noise performance, and increased bandwidth. InvCas TIA allows less direct current (DC) current which yields low power consumption. An existing basic InvCas TIA circuit diagram is illustrated in Figure 2.

The circuit diagram of the proposed wideband TIA with bandwidth tuning is exhibited in Figure 3. The first stage is a modified InvCas TIA with the inductive peaking provided at the input terminal and the feedback loop in parallel with a series combination of feedback capacitor and the feedback resistor. The series peaking inductors and the shunt peaking inductors are used to realize the resonance with the feedback capacitor and the parasitic capacitance of the InvCas amplifier. Hence, the bandwidth of the input side of the amplifier is extended.

Table 1 describes the transistor sizes. The cascode-transistors M_{N2} and M_{P2} in the InvCas TIA provide improvement of the gain bandwidth product (GBW) compared to the Inv-TIA. The sources of the cascode-transistors M_{N2} and M_{P2} are connected to the drains of the transistors M_{N1} and M_{P1} respectively in the InvCas TIA. As a result, the input side's miller capacitance is decreased. The resistances through the drains of M_{N1} are equal to g_{mN2}^{-1} and M_{P1} is g_{mP2}^{-1} .

Stage 2 is a common-source amplifier with a shunt-peaking inductor and a miller-cap arrangement. This novel technique is used to extend the bandwidth. Inductive-peaking is used to enhance the amplifier's bandwidth. In series-peaking technique, an inductor is connected in series with the input-signal. Similarly, in the shunt-peaking technique, the peaking inductor is connected in parallel to the load capacitor. The gain is a product of transconductance and the trans-impedance. The transconductance is a constant whereas the trans-impedance can be varied. Table 2 explains component values. The transfer-function of the InvCas TIA is illustrated in (1).

$$Z(s)_{TF} = \frac{V_{out}}{I_{in}} = \frac{1}{sC} \parallel (R + sL) = \frac{R+sL}{1+sRC+LCs^2} \quad (1)$$

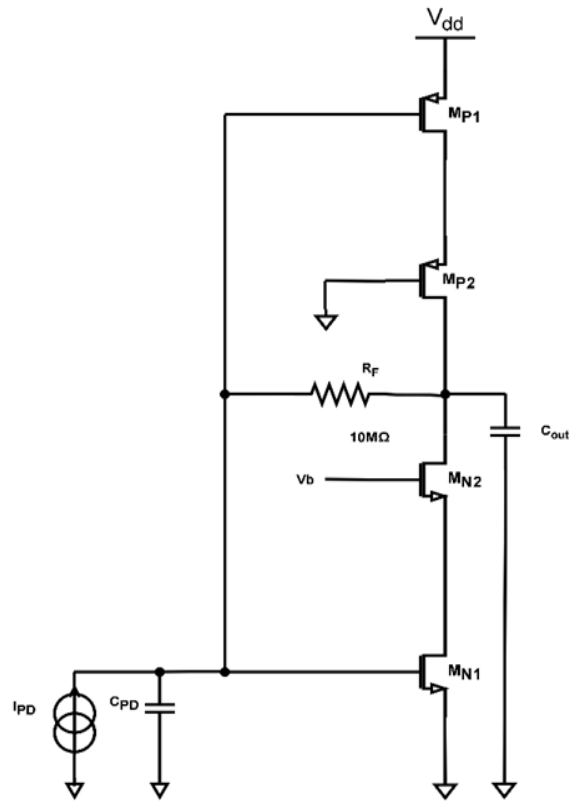


Figure 2. Existing basic InvCas TIA

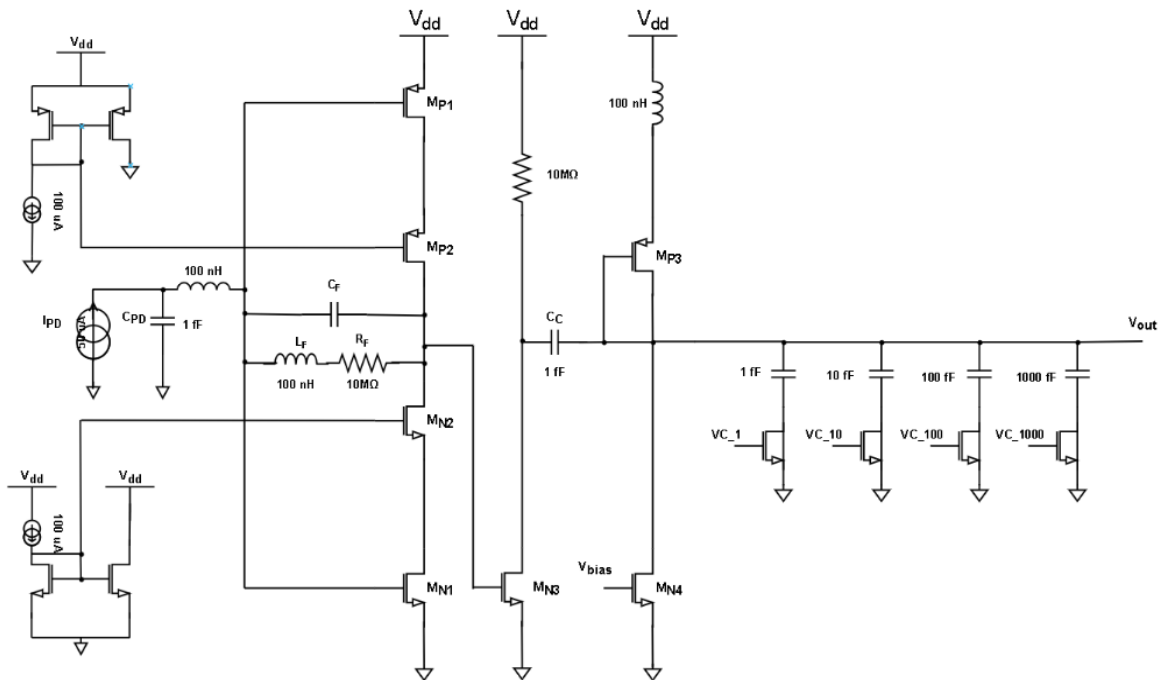


Figure 3. Proposed wideband TIA with bandwidth tuning

Table 1. Transistor sizes

Transistors	W/L (μm)
M_{N1}	20/1
M_{N2}	2/1
M_{P1}	20/1
M_{P2}	2/1
M_{N3}	40/1
M_{N4}	10/1
M_{P3}	5/1

Table 2. Component values

Component	Values
I_{PD}	10-50 μA
C_{PD}	1 fF
Ind_{in}	100 nH
Ind_F	100 nH
C_F	1 fF
R_F	10 M Ω
R_D	10 M Ω
C_C	1 fF
C_{T1}	1 fF
C_{T10}	10 fF
C_{T100}	100 fF
C_{T1000}	1,000 fF

The peaking inductor introduces a “zero” in the $Z(s)_{TF}$. The reactive impedance of the inductor compensates the reactive impedance of the capacitor and thus the amplifier’s bandwidth is increased or enhanced. The output node is connected to a hybrid load capacitor bank which is a combination of fixed capacitors and tunable MOS capacitors. The capacitor bank has four branches. The first branch has a 1fF fixed capacitor and a tunable MOS capacitor. The second branch has a 10 fF fixed capacitor and a tunable MOS capacitor. The third branch has a 100 fF fixed capacitor and a tunable MOS capacitor. The fourth branch has a 1,000 fF fixed capacitor and a tunable MOS capacitor. Each branch has dedicated tuning control signals V_{C_1} , V_{C_10} , V_{C_100} , V_{C_1000} for the 1st branch, 2nd second branch, 3rd branch and 4th branch respectively. V_{C_1} is used to tune the 1 fF capacitor, V_{C_10} is used to tune the 10 fF capacitor, V_{C_100} is used to tune the 100 fF capacitor and V_{C_1000} is used to tune the 1,000 fF capacitor.

The control signals (V_{C_1} , V_{C_10} , V_{C_100} , V_{C_1000}) can be varied individually for small variations or together for major variations in the bandwidth. A similar capacitor bank arrangement can be used instead of the photo-diode capacitance C_{PD} on the input side. When the V_{C_1} control signal is varied, the change in the capacitance will be in the range of a portion of a femto-Farad and the maximum branch capacitance is 1 fF. Similarly, the other branch capacitances can also be varied. By increasing the load capacitance, the location of the dominant pole is moved to the left side in the frequency spectrum and vice-versa. Thus, the bandwidth tuning is achieved by load capacitor tuning in this proposed TIA architecture.

The output-resistance of the proposed TIA is calculated by (2). Where, g_{mN2} , g_{mP2} are the transconductance of M_{N2} and M_{P2} and r_{oN1} , r_{oN2} , r_{oP1} and r_{oP2} are output -resistance of M_{N1} , M_{N2} , M_{P1} and M_{P2} respectively. The open loop gain of the proposed TIA can be calculated by (3). The total transconductance to calculate the open-loop gain is calculated by (4). The input-resistance at zero-frequency is calculated by (5). Where, R_{out} is output resistance of the TIA and R_F is feedback resistor of the TIA. The bandwidth of the proposed TIA can be calculated by (6).

$$R_{out} = \left(g_{mN2} + \frac{1}{r_{oN1}} + \frac{1}{r_{oN2}} \right) r_{oN1} r_{oN2} \parallel \left(g_{mP2} + \frac{1}{r_{oP1}} + \frac{1}{r_{oP2}} \right) r_{oP1} r_{oP2} \quad (2)$$

$$A_{Inv_Cas} = -G_m R_{out} \quad (3)$$

$$G_m = g_{mN1} + g_{mP1} \quad (4)$$

$$Z(0)_{in} = \frac{R_{out} + R_F}{-G_m R_{out} + 1} \quad (5)$$

$$Bandwidth = \frac{G_m R_{out} + 1}{2\pi(R_{out} + R_F)(C_{out} + C_{PD})} \quad (6)$$

2.2. Common-source amplifier

The second stage of the proposed TIA is the common-source amplifier to enhance the amplified signal further to a few hundred millivolts. The common-source amplifier's gain is calculated by (7). Where, g_{mN3} is the transconductance of the transistor used in common-source amplifier, R_D is drain-resistance of the common-source amplifier. The Miller capacitor C_C is used in the second stage of the WBTIA to extend the bandwidth. The pole introduced by the Miller-effect is shifted towards a higher frequency which increases the bandwidth.

$$A_{CS} = -g_{mN3}R_D \quad (7)$$

2.3. Buffer amplifier

The buffer amplifier is used in the output side of the proposed TIA after the second stage amplifier. It isolates two stages, where the output of the buffer is connected to the input of the second circuit and the input of the buffer is connected to the output of the first circuit. Buffer amplifier has the following advantages such as low output-impedance, high input-impedance and high bandwidth. The buffer amplifier has a unity gain and high bandwidth. Buffer amplifier passes all range of frequencies without any attenuation. The schematic diagram of the unity gain buffer-amplifier is depicted in Figure 4.

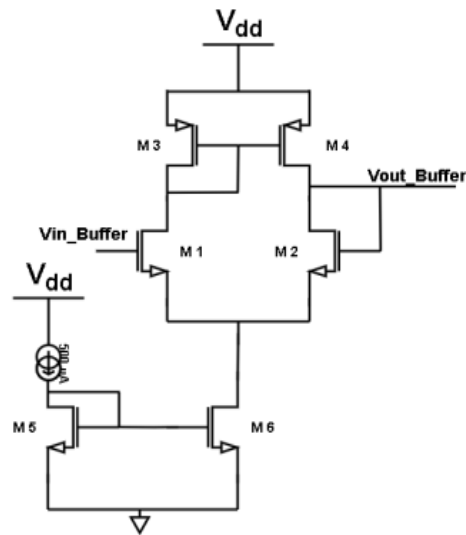


Figure 4. Buffer amplifier

2.4. High pass filter

The third stage of the proposed TIA is the tunable HPF with a lower cut-off frequency which allows all other higher frequencies. The output signal from the buffer amplifier is passed through the HPF filter with a predetermined cutoff-frequency (f_{c_HPF}). The cutoff-frequency of the HPF is calculated by the (8).

$$\text{HPF cut-off frequency } f_{c_HPF} = \frac{1}{2\pi R_{HPF} C_{HPF}} \quad (8)$$

2.5. Low-pass filter

The fourth stage of the proposed TIA is the tunable LPF with a higher cut-off frequency which allows till the predetermined frequency. The output signal from the HPF is passed through the LPF filter with a predetermined cutoff-frequency (f_{c_LPF}). The cutoff-frequency of the LPF can be calculated by (9).

LPF cut-off frequency

$$f_{c_LPF} = \frac{1}{2\pi R_{LPF} C_{LPF}} \quad (9)$$

The HPF is designed for 5 kHz and the LPF is designed for 100 MHz to select the frequency band used for NIRS biomedical applications. Both HPF and LPF can be designed to any cutoff frequency and the

required band of frequency will be allowed to pass through and the other frequency will be attenuated. Thus, the required bandwidth can be selected by tuning the R and C values of the HPF and LPF. Figures 5(a) and 5(b) illustrates the schematic diagrams of HPF and LPF.

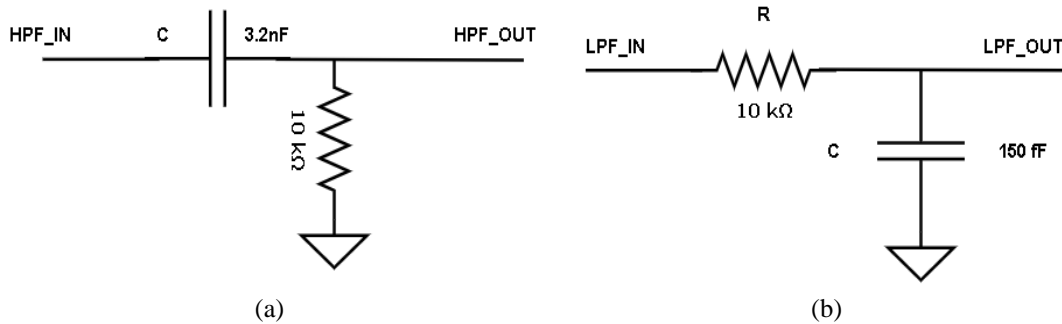


Figure 5. Illustrates the schematic diagrams of (a) HPF and (b) LPF

2.6. Band-pass filter

The tunable HPF with a lower cutoff frequency and the tunable LPF with a higher cutoff frequency. Both form the tunable band-pass filter (BPF). By tuning the BPF to the required range of frequencies, any interested frequency band can be selected by the proposed TIA within the range of frequencies (1 kHz to 354 MHz) supported by the proposed TIA.

3. RESULTS AND DISCUSSION

The proposed wideband TIA with bandwidth tuning is designed and simulated using generic process design kit (GSDK) 45 nm technology node. Simulations are performed using cadence analog design environment (ADE). The input photo-current from the photo-diode and the output-voltage of the proposed TIA after the second stage is plotted in Figure 6.

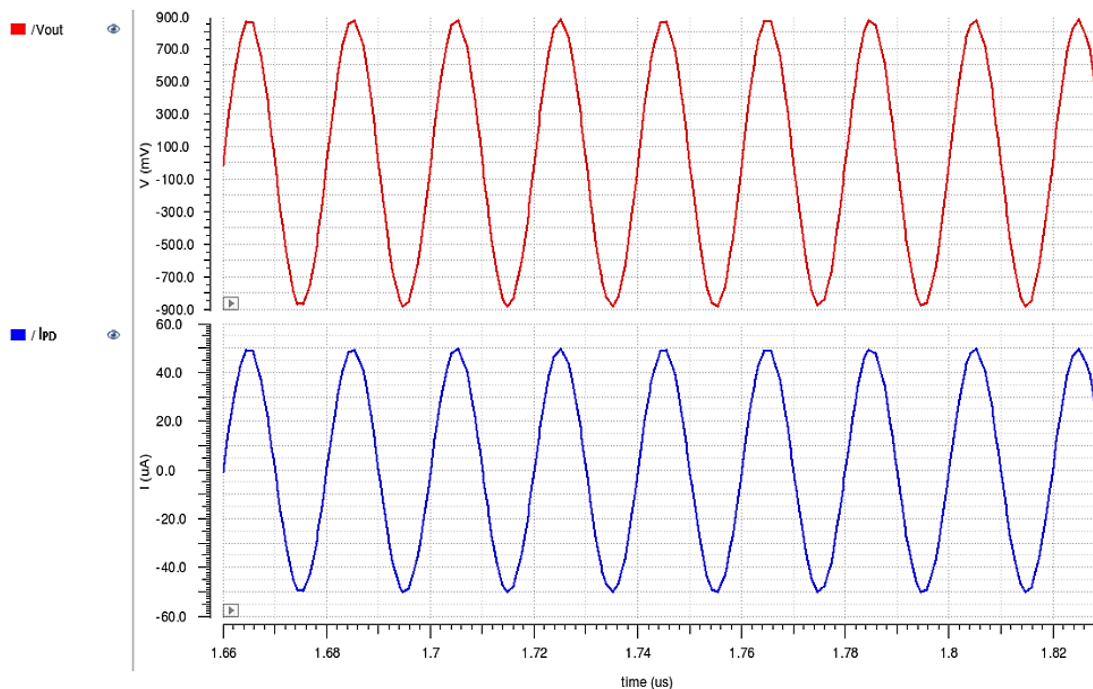


Figure 6. Input photo-current and output-voltage of the proposed TIA

The input photo-current is 50 μA and the output voltage is 880 mV. The TIG of the WB TIA is 84.91 dB Ω . The AC analysis of the WB TIA is performed from 1 kHz to 1 GHz. The WB TIA exhibits 84.91 dB Ω gain and 354.81 MHz bandwidth. The GBW is 30126.91. The proposed TIA outperforms the other similar architectures in the literature. The phase margin is 103.44°. The proposed TIA has a single dominant pole at a higher frequency and a high phase margin. Hence, the proposed TIA has high stability. The dominant pole is located at 100 MHz. The frequency response of the proposed wideband TIA is plotted in Figure 7. The influence of tuning control voltage on the load capacitance is illustrated in Figure 8. The value of the load capacitance increases as the tuning control voltage increases. When the control voltage is 100 mV the load capacitance is 35 fF and it reaches 100 fF when the control voltage reaches 1 V.

The impact of the tuning capacitor on the bandwidth is shown in Figure 9. The change in the bandwidth is inversely proportional to the load capacitance. When the load tuning capacitor is 10 fF the bandwidth is 240 MHz and it reaches 60 MHz when the load capacitance is 100 fF. The achieved bandwidths for the different load capacitors 1 fF, 5 fF, and 10 fF are depicted in Figure 10. The location of the dominant pole is changed by changing the value of C_{out} to get the required bandwidth. The location of the dominant poles for different load capacitances is shown by the three green dots. Thus, the bandwidth tuning is achieved by varying the C_{out} . Dominant pole locations for 1 fF, 5 fF, and 10 fF are 60, 11, and 10 MHz respectively. Input referred noise current is calculated by (10).

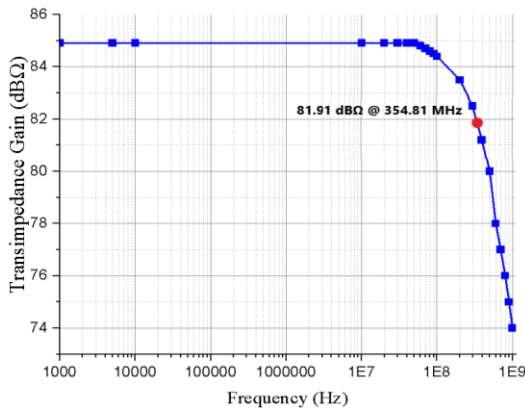


Figure 7. Frequency response of the proposed TIA

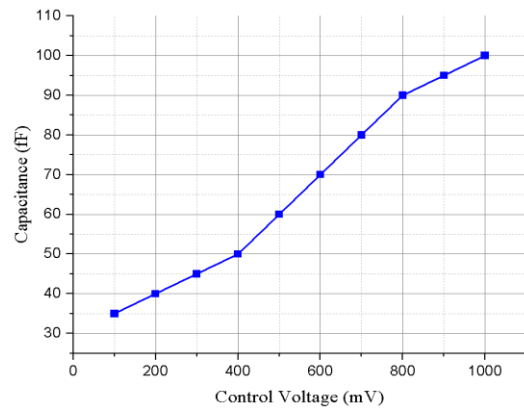


Figure 8. Control voltage vs tuning capacitor

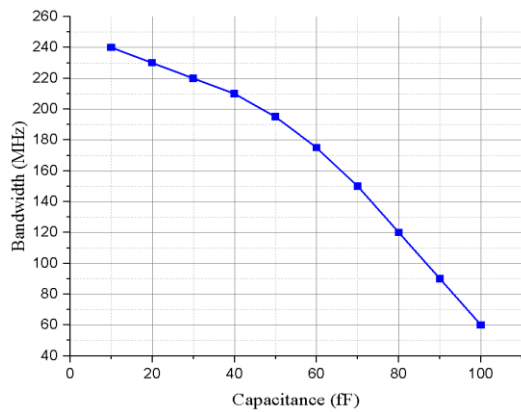


Figure 9. Impact of tuning capacitor on bandwidth

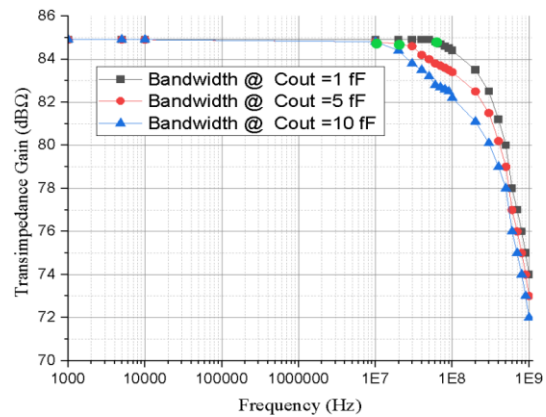


Figure 10. Impact of load capacitor bandwidth

$$I_{n,in}^2 = 4K_B T \left[\frac{(G_m^2 + (2\pi f C_{PD})^2)}{(1 - G_m R_F)^2} R_F + \frac{(1 + (2\pi f C_{PD} R_F)^2)}{(1 - G_m R_F)^2} ((g_{mN1} \gamma_n + g_{mP1} \gamma_p)) + \frac{(1 + (2\pi f C_{PD} R_F)^2)}{(1 - G_m R_F)(g_{mN2} + \frac{1}{r_{oN2}}) r_{oN1}} g_{mN2} \gamma_n + \frac{(1 + (2\pi f C_{PD} R_F)^2)}{(1 - G_m R_F)(g_{mP2} + \frac{1}{r_{oP2}}) r_{oP1}} g_{mP2} \gamma_p + f \times R_F \right] \quad (10)$$

The first term belongs to the input-noise due to the feedback resistor, and the second term is the input-referred noise from M_{N1} and M_{P1} . The third is the contribution of M_{N2} and the fourth term is the contribution of M_{P2} . The last term is the noise contribution due to the thermal noise of the series resistance of the inductor. The frequency response of the input-referred noise current is plotted in Figure 11 and the frequency response of the output-voltage noise is illustrated in Figure 12. The input-referred noise current exponentially increases as the frequency is increased. The input-referred noise current of the WBTIA at 100 MHz is 169 fA/sqrt(Hz) which is much less compared to the other architecture [19] in the literature.

The output-noise voltage exponentially decreases as the frequency increases till 100 kHz and becomes constant after that. The output-noise voltage of the WBTIA is 69.8 pV/sqrt(Hz). The Monte Carlo simulation of the bandwidth variation is shown in Figure 13. Total no of samples taken is 100. The average bandwidth is 300 MHz and the standard deviation is 45 MHz from 354.81 MHz. The impact of power supply voltage on power consumption is illustrated in Figure 14.

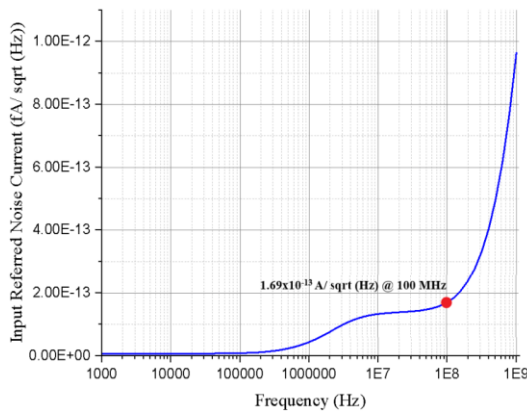


Figure 11. Frequency response of input referred noise current

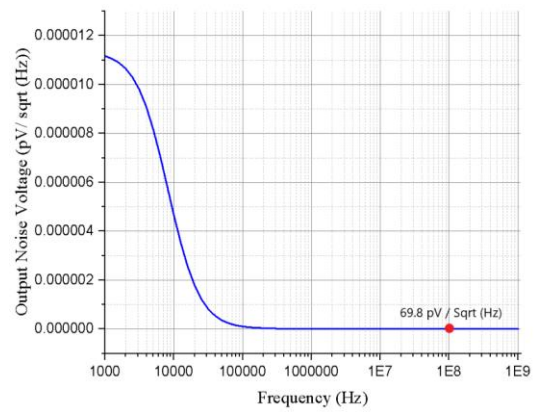


Figure 12. Frequency response of output noise voltage

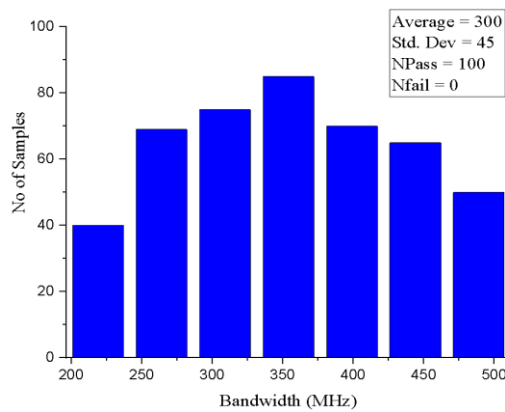


Figure 13. Monte Carlo simulation of bandwidth variation

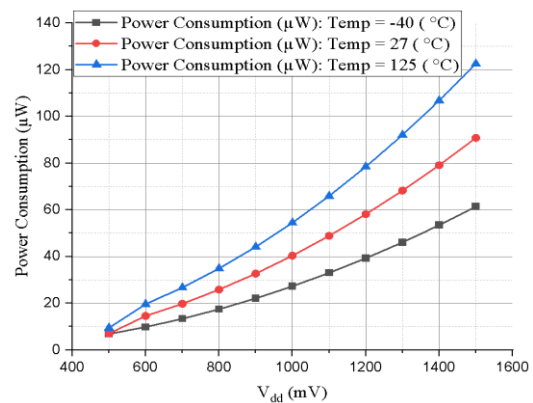


Figure 14. Impact of power supply on power consumption

The power supply is changed from 500 to 1,500 mV for various temperatures such as -40 °C, 27 °C, and 125 °C. The proposed TIA consumes 41.24 µW at 27 °C and 1 V supply. From the graph, it is observed that the power consumption is huge when both the temperature and the supply voltage are high and vice versa. The layout of the WBTIA is illustrated in Figure 15. The proposed wideband TIA occupies a layout area of 12.395×12.415 µm. The performance parameters of the various TIAs in the literature are enumerated in Table 3. The proposed TIA outperforms well compared to the other TIAs in the literature [19], [21] in terms of input-referred noise current, trans-impedance gain, bandwidth tuning range, and power consumption.

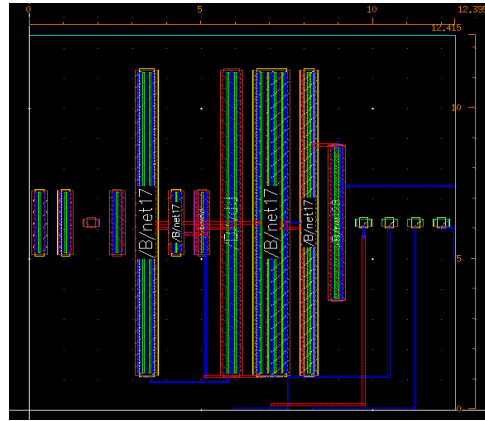


Figure 15. Layout diagram of the proposed wideband TIA with tuning

Table 3. Performance comparison

Description	[18]	[19]	[21]	[24]	[25]	Our Work
Technology (nm)	180	180	180	45	45	45
Trans-impedance gain (dBΩ)	47.8	39.8	26	68.5	100	84.91
Bandwidth	6.2-10.5 GHz	0.1-300 Hz	100 MHz	8.9 GHz	25 MHz	1 kHz-354.81 MHz
Input noise current	-	200 nA/√Hz	-	1.274 μA/√Hz	-	169 fA/√Hz
Output noise voltage	-	20nV/√Hz	-	-	-	69.8 pV/√Hz
Supply voltage (V)	1.8	1.8	1.8	1	1	1
Power	33.33 mW	54μW	125 μW	37 mW	12 μW	41.24 μW
Tuning technique	Capacitor	Pseudo-resistor	Feedback resistor	Load Resistor	Capacitor	Inductive peaking and MOS cap
Layout area	0.9x0.6 mm×mm	-	0.054×0.054 mm×mm	0.49×0.49 mm×mm	0.07×0.07 mm×mm	12.395×12.415 μm x μm

4. CONCLUSION

In this research article, a Wideband TIA with bandwidth tuning is proposed and implemented using 45 nm technology for NIRS bio-medical applications. Bandwidth tuning is achieved by a novel tuning mechanism with a fixed capacitor and tunable metal–oxide–semiconductor capacitor with a control voltage. The fixed capacitor provides a coarse-grain bandwidth tuning whereas the tunable MOS capacitors are used for fine-grain bandwidth tuning. By changing the control voltage of the tuning load capacitor, the bandwidth of the proposed WBTIA is varied, while maintaining a transimpedance gain of 84.91 dBΩ. The proposed WBTIA achieved -3 dB bandwidth of 354.81 MHz. The proposed WBTIA consumes 41.24 μW power from 1 V supply voltage at the temperature of 27 °C. The input-referred current noise and the output noise voltage at 100 MHz are 169 fA/sqrt (Hz) and 69.8 pV/sqrt (Hz) respectively. The layout area of the proposed TIA is 12.395×12.415 μm.

ACKNOWLEDGEMENT

This work was supported by Visvesvaraya PhD Scheme, Ministry of Electronics and Information Technology (MeitY), Government of India. VISPHD-MEITY-3062.




REFERENCES

- [1] A. Atef, M. Atef, E. E. M. Khaled, and M. Abbas, "CMOS transimpedance amplifiers for biomedical applications: a comparative study," *IEEE Circuits and Systems Magazine*, vol. 20, no. 1, pp. 12–31, 2020, doi: 10.1109/MCAS.2019.2961724.
- [2] Y. Yoon, J. H. Cho, and G. Yoon, "Non-constrained blood pressure monitoring using ECG and PPG for personal healthcare," *Journal of Medical Systems*, vol. 33, no. 4, pp. 261–266, 2009, doi: 10.1007/s10916-008-9186-0.
- [3] J. E. Naschitz *et al.*, "Pulse transit time by r-wave-gated infrared photoplethysmography: review of the literature and personal experience," *Journal of Clinical Monitoring and Computing*, vol. 18, no. 5–6, pp. 333–342, 2004, doi: 10.1007/s10877-005-4300-z.
- [4] G. Wang, M. Atef, and Y. Lian, "Towards a continuous non-invasive cuffless blood pressure monitoring system using PPG: systems and circuits review," *IEEE Circuits and Systems Magazine*, vol. 18, no. 3, pp. 6–26, 2018, doi: 10.1109/MCAS.2018.2849261.
- [5] J. Yadav, A. Rani, V. Singh, and B. M. Murari, "Near-infrared LED based non-invasive blood glucose sensor," *2014 International Conference on Signal Processing and Integrated Networks, SPIN 2014*, 2014, pp. 591–594, doi: 10.1109/spin.2014.6777023.




- [6] R. Pandey *et al.*, “Noninvasive monitoring of blood glucose with Raman spectroscopy,” *Accounts of Chemical Research*, vol. 50, no. 2, pp. 264–272, 2017, doi: 10.1021/acs.accounts.6b00472.
- [7] F. F. Jöbsis, “Noninvasive, infrared monitoring of cerebral and myocardial oxygen sufficiency and circulatory parameters,” *Science*, vol. 198, no. 4323, pp. 1264–1266, 1977, doi: 10.1126/science.929199.
- [8] T. Jue and K. Masuda, “Application of near infrared spectroscopy in biomedicine,” *Application of Near Infrared Spectroscopy in Biomedicine*, pp. 1–151, 2013, doi: 10.1007/978-1-4614-6252-1.
- [9] O. J. Arthurs and S. J. Boniface, “What aspect of the fMRI BOLD signal best reflects the underlying electrophysiology in human somatosensory cortex?,” *Clinical Neurophysiology*, vol. 114, no. 7, pp. 1203–1209, 2003, doi: 10.1016/S1388-2457(03)00080-4.
- [10] M. S. Reis, D. C. Berton, R. Arena, A. M. Catai, J. A. Neder, and A. Borghi-Silva, “Determination of anaerobic threshold through heart rate and near infrared spectroscopy in elderly healthy men,” *Brazilian Journal of Physical Therapy*, vol. 17, no. 5, 2013, doi: 10.1590/S1413-35552012005000115.
- [11] K. Schneider and H. Zimmermann, “Highly sensitive optical receivers,” *Springer Series in Advanced Microelectronics*, vol. 23, pp. 1–193, 2006, doi: 10.1007/978-3-540-29614-0_1.
- [12] F. Aflatouni and H. Hashemi, “A 1.8mW wideband 57 dBΩ trans-impedance amplifier in 0.13 μm CMOS,” *2009 IEEE Radio Frequency Integrated Circuits Symposium*, pp. 57–60, 2009, doi: 10.1109/RFIC.2009.5135489.
- [13] S. M. Park, “A 16-channel CMOS inverter transimpedance amplifier array for 3-D image processing of unmanned vehicles,” *Transactions of the Korean Institute of Electrical Engineers*, vol. 64, no. 12, pp. 1730–1736, 2015, doi: 10.5370/KIEE.2015.64.12.1730.
- [14] J. Tak, H. Kim, J. Shin, J. Lee, J. Han, and S. M. Park, “A low-power wideband trans-impedance amplifier in 0.13 μm CMOS,” in *2011 IEEE MTT-S International Microwave Workshop Series on Intelligent Radio for Future Personal Terminals*, 2011, pp. 1–2.
- [15] M. Atef, H. Chen, and H. Zimmermann, “10 Gb/s inverter based cascode trans-impedance amplifier in 40nm CMOS technology,” *2013 IEEE 16th International Symposium on Design and Diagnostics of Electronic Circuits & Systems (DDECS)*, pp. 72–75, 2013, doi: 10.1109/DDECS.2013.6549791.
- [16] A. Atef, M. Atef, M. Abbas, and E. E. M. Khaled, “High-sensitivity regulated inverter cascode trans-impedance amplifier for near-infrared spectroscopy,” in *2016 Fourth International Japan-Egypt Conference on Electronics, Communications and Computers (JEC-ECC)*, 2016, pp. 99–102, doi: 10.1109/JEC-ECC.2016.7518977.
- [17] C. Toumazou and S. M. Park, “Wideband low noise CMOS transimpedance amplifier for gigaHertz operation,” *Electronics Letters*, vol. 32, no. 13, pp. 1194–1196, 1996, doi: 10.1049/el:19960814.
- [18] C. K. Chien, H. H. Hsieh, H. S. Chen, and L. H. Lu, “A transimpedance amplifier with a tunable bandwidth in 0.18-μm CMOS,” *IEEE Transactions on Microwave Theory and Techniques*, vol. 58, no. 3, pp. 498–505, 2010, doi: 10.1109/TMTT.2010.2040328.
- [19] S. Hwang, K. Aninakwa, and S. Sonkusale, “Bandwidth tunable amplifier for recording biopotential signals,” in *2010 Annual International Conference of the IEEE Engineering in Medicine and Biology Society, EMBC’10*, 2010, pp. 662–665, doi: 10.1109/IEMBS.2010.5627215.
- [20] M. M. R. Ibrahim and P. M. Levine, “CMOS transimpedance amplifier for biosensor signal acquisition,” in *Proceedings - IEEE International Symposium on Circuits and Systems*, 2014, pp. 25–28, doi: 10.1109/ISCAS.2014.6865056.
- [21] M. A. S. Bhuiyan, M. I. B. Idris, M. B. I. Reaz, K. N. Minhada, and H. Husain, “Low voltage and wide bandwidth class AB variable gain amplifier in 0.18-μm CMOS technology,” *Przeglad Elektrotechniczny*, vol. 90, no. 6, 2014, doi: 10.12915/pe.2014.06.34.
- [22] M. Mathew, B. L. Hart, and K. Hayatleh, “Low input-resistance low-power transimpedance amplifier design for biomedical applications,” *Analog Integrated Circuits and Signal Processing*, vol. 110, no. 3, pp. 527–534, 2022, doi: 10.1007/s10470-021-01985-x.
- [23] G. Royo, M. Garcia-Bosque, C. Sánchez-Azqueta, C. Aldea, S. Celma, and C. Gimeno, “Transimpedance amplifier with programmable gain and bandwidth for capacitive MEMS accelerometers,” 2017, doi: 10.1109/I2MTC.2017.7969937.
- [24] W. Liao, C. Chen, D. Gao, and Y. Huang, “A 10Gbps high-speed low-noise optical receiver based on CMOS 45nm technology,” 2023, doi: 10.1109/ASICON58565.2023.10395952.
- [25] R. Nagulapalli, S. Zourob, K. Hayatleh, N. Yassine, S. Barker, and A. Venkatarreddy, “A compact high gain opamp for Bio-medical applications in 45nm CMOS technology,” in *RTEICT 2017 - 2nd IEEE International Conference on Recent Trends in Electronics, Information and Communication Technology, Proceedings*, 2017, vol. 2018-Janua, pp. 231–235, doi: 10.1109/RTEICT.2017.8256592.

BIOGRAPHIES OF AUTHORS



Muthukumar Balasubramanian    received a B.E. degree in electronics and Communication engineering from Madras Institute of Science and Technology, Chennai in 2008 and an M.E. degree in applied electronics in 2012 from Sathyabama University Chennai. Currently, he pursuing PhD in the area of VLSI, he is an assistant professor at the Department of Electronics and Communication Engineering, SRM Institute of Science and Technology, Chennai. His research interests include optical communication, VLSI, and analog circuits. He can be contacted at email: muthukub1@srmist.edu.in.



Ramachandran Balasubramanian    received a B.E. degree in electronics and communication engineering from Thiagarajar College of Engineering, Madurai Kamarajar University, Madurai in 1990 and an M.E. degree in satellite communications 1992 from Regional Engineering College (Presently NIT), Bharathidasan University, Trichy and PhD degree in wireless and mobile networks. College of Engineering Guindy, Anna University. Currently, he is a professor at the Department of Electronics and Communication Engineering, SRM Institute of Science and Technology, Chennai. His research interests include Adhoc and sensor networks, next generation networks, cross layer designs, baseband signal processing, and antenna design. He can be contacted at email: ramachab@srmist.edu.in.